



Killat, N., Pomeroy, J. W., Jimenez, J. L., & Kuball, M. H. H. (2014). Thermal properties of AlGa_N/Ga_N high electron mobility transistors on 4H and 6H SiC substrates. *physica status solidi (a)*, 211(12), 2844-2847. DOI: 10.1002/pssa.201431440

Peer reviewed version

Link to published version (if available):
[10.1002/pssa.201431440](https://doi.org/10.1002/pssa.201431440)

[Link to publication record in Explore Bristol Research](#)
PDF-document

This is the author accepted manuscript (AAM). The final published version (version of record) is available online via Wiley at <http://onlinelibrary.wiley.com/doi/10.1002/pssa.201431440/abstract>.

University of Bristol - Explore Bristol Research

General rights

This document is made available in accordance with publisher policies. Please cite only the published version using the reference above. Full terms of use are available:
<http://www.bristol.ac.uk/pure/about/ebr-terms.html>

Thermal properties of AlGaIn/GaN high electron mobility transistors on 4H and 6H SiC substrates

Nicole Killat ^{*1}, James W. Pomeroy¹, Jose L. Jimenez², and Martin Kuball ^{**1}

¹ Center for Device Thermography and Reliability, University of Bristol, H.H. Wills Physics Laboratory, Tyndall Avenue, BS8 1TL Bristol, United Kingdom

² TriQuint Semiconductor Inc., Richardson TX 75080, United States

Received ZZZ, revised ZZZ, accepted ZZZ

Published online ZZZ(Dates will be provided by the publisher.)

Keywords: Thermal conductivity, SiC substrate, AlGaIn/GaN HEMT, Raman thermography.

* Corresponding author: e-mail Nicole.Killat@bristol.ac.uk, Phone: +44 (0)117 33 18110, Fax: +44 (0)117 925 5624

** e-mail martin.kuball@bristol.ac.uk, Phone: +44 (0)1179288734

Micro-Raman thermography was employed to study the difference in thermal properties of identical, state-of-the-art AlGaIn/GaN devices grown onto 4H SiC and 6H SiC substrates. Using temperature profiles in the devices taken laterally across the device surface and vertically through the device structure of multiple devices, a 10% higher peak temperature for AlGaIn/GaN transistors on 6H SiC when compared to devices on 4H SiC was found. The comparison of experimental temperature with three-

dimensional finite difference thermal simulations determined a room temperature thermal conductivity of $4.1 \text{ W cm}^{-1} \text{ K}^{-1}$ and $4.5 \text{ W cm}^{-1} \text{ K}^{-1}$ for devices on the studied 6H and 4H SiC, respectively, as underlying physical reason for this temperature difference, while the thermal boundary resistance between the GaN and the SiC were identical within the experimental error bar for both GaN-on-SiC wafers, independent on polytype.

Copyright line will be provided by the publisher

1 Introduction With the recent advances in manufacturing and technology, AlGaIn/GaN high electron mobility transistors (HEMTs) have received increasing attention for high power, high frequency applications within the radar, communications, and automotive sector [1, 2]. With a growing range of applications, reliability issues still pose limitations for this technology. Thermal management in AlGaIn/GaN HEMTs is here of particular concern, since Joule self-heating in the region of high electric field next to the gate contact can lead to a significant temperature rise in the active device area. Considering the thermally induced device degradation including the impact of temperature rise on charge trapping and defect generation, the knowledge of device temperature and the subsequent improvement of thermal management are essential to achieve long device lifetimes in AlGaIn/GaN HEMTs.

For GaN-based HEMTs, SiC presents the foreign substrate of choice. This is primarily accredited to its high electrical resistivity and small lattice mismatch to GaN, but in particular due to its high thermal conductivity when

compared to Si or sapphire substrates [3, 4]. Consequently, SiC is ideally suited as substrate material for GaN devices for high frequency and high power applications. Nevertheless, thermal conductivity depends on many factors such as defect and dislocation density, layer thickness, growth quality, and in particular its polytype. The polytypes 4H SiC and 6H SiC are predominantly used for GaN-based devices. With the development of AlGaIn/GaN HEMTs, 4H SiC has become a favourable substrate material, with extensive research and development achieving technology improvements [4, 5], raising the question on whether this is also the thermally most efficient SiC polytype. For both SiC polytypes, literature values for room temperature thermal conductivity vary between 3 and 5 W/cmK with strong temperature dependencies between $T^{-0.5}$ and T^{-3} , however, this is mostly historic experimental data, where many of its thermal properties were still strongly impacted by material imperfections, as reported in Refs. [6-9] and references therein. Müller et al. reported a 10% difference in experimentally estimated thermal conductivity values of

Copyright line will be provided by the publisher

n-type 4H SiC ($3.3 \text{ W cm}^{-1} \text{ K}^{-1}$) and 6H SiC ($3.0 \text{ W cm}^{-1} \text{ K}^{-1}$) for similar carrier concentration ($\sim 10^{18} \text{ cm}^{-3}$) and growth direction [10], however, a high thermal conductivity of insulating state-of-the-art substrates is needed for GaN-based microwave devices. Others claim no difference in thermal conductivity between 4H SiC and 6H SiC with numbers reported up to $4.9 \text{ W cm}^{-1} \text{ K}^{-1}$ [11]. Although the thermal properties of SiC crystals have been extensively studied, a conclusion on the difference between 4H SiC and 6H SiC and more importantly the final effects on GaN device thermal properties remain unclear. In this work, a direct comparison of the thermal properties of identical AlGaN/GaN devices grown on state-of-the-art 4H SiC and 6H SiC substrates is presented. Device temperature data estimated by micro-Raman thermography on operating devices were compared with thermal simulations to validate the thermal properties of the two SiC polytypes.

2 Experimental details

Identical AlGaN/GaN device structures were grown on 100- μm -thick 4H SiC and 6H SiC substrates by metal organic vapor deposition (MOCVD), using a 1.8- μm -thick GaN buffer and a 21-nm-thin AlGaN barrier layer. Ungated AlGaN/GaN HEMTs with a 16- μm -wide gap and 100- μm -wide ohmic contacts were fabricated and passivated with a SiN_x layer. The devices were mesa-isolated. Ungated HEMTs have been shown to enable the access to information on key thermal parameters of this device system [3, 12]. The temperature profile was assessed on ungated HEMTs with standard Ohmic contacts by means of micro-Raman thermography. This optical, non-invasive method of temperature assessment utilises a laser beam at a wavelength of 488 nm combined with a Renishaw inVia spectrometer and a $50\times$ ($\text{NA} = 0.5$) objective to probe phonon modes in the crystal. The GaN $A_1(\text{LO})$ phonon mode and the SiC E_2 -type mode were used to determine the temperature of these respective materials. More details on the technique can be found in Ref. 3. Both temperature profiles recorded in the center of the device from the device surface into the SiC substrate, and laterally in the GaN, from the centre of the device to outside the active device region, were considered. The device back-plate temperature was kept at 25°C using a Peltier-cooled thermal stage. A lateral resolution of $\sim 0.6 \mu\text{m}$ was achieved, while the depth resolution based on confocal microscopy was $\sim 5 \mu\text{m}$ near the interface in the SiC, or the GaN layer thickness, respectively [3, 13-16].

The Raman temperature results were compared with three-dimensional (3D) finite-difference thermal simulations using a standard thermal analysis system (TAS) and ANSYS. The device and layer structure was set up in the thermal model, as experimentally studied here. The thermal properties of the SiC substrate were varied in the thermal model, assuming anisotropic thermal conductivity, as is often used in device thermal simulations [17]. For the GaN epilayer a thermal conductivity of $1.6 \text{ W cm}^{-1} \text{ K}^{-1}$

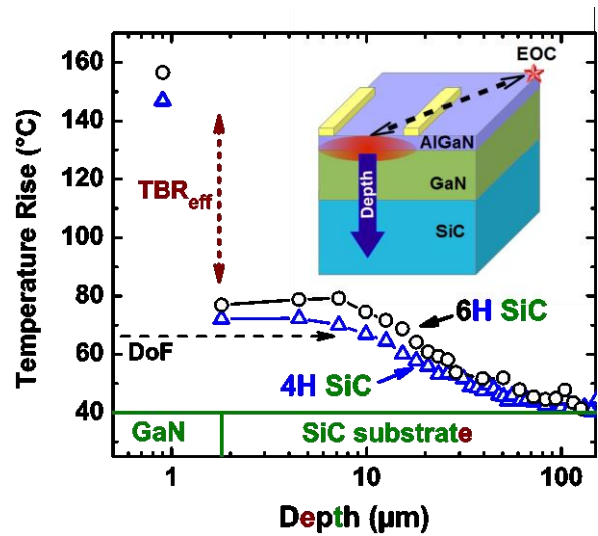


Figure 1 Raman temperature rise versus depth of two identical AlGaN/GaN devices on 6H SiC and 4H SiC, respectively. The devices were operated at a power density of 30 W/mm^2 and a back-plate temperature of 25°C . The TBR_{eff} (effective thermal boundary resistance) at the GaN-SiC interface and the depth of field (DoF) are indicated. The inset illustrates the temperature scan from the device surface through the substrate as well as the edge of chip (EOC) temperature measurement position.

with a temperature dependence of $T^{-1.4}$ was implemented [13]. For the ungated HEMT a uniform heat source on the device surface was considered.

3 Results and Discussion

Figure 1 displays the temperature profile in the centre of a representative ungated AlGaN/GaN HEMT recorded by micro-Raman thermography. The profile was acquired from the device surface vertically into the SiC substrate, as illustrated in the inset of Fig. 1, for identical devices on 4H and 6H SiC, respectively. The devices were operated at identical power dissipation. The temperature rise with respect to the edge of chip (EOC) temperature was measured $\sim 700 \mu\text{m}$ away from the device centre (see inset in Fig. 1), which is used to account for possible chip-to-chip differences in thermal resistance between the back of the chip and the heat sink. For both cases, i.e., 4H and 6H SiC substrate, the temperature profile exhibits a noticeable temperature step at the GaN-SiC interface. This temperature step arises due to the thermal resistance of the GaN-SiC interface, often termed as effective thermal boundary resistance (TBR_{eff}). This phenomenon is associated to the nucleation layer at the GaN-SiC interface and to defects near this interface [12, 14]. Figure 1 illustrates that TBR_{eff} of the GaN-SiC interface, which will be quantified later, was identical in both devices under investigation within the experimental accuracy, illustrating that the epitaxial growth of GaN onto 4H or 6H SiC substrates can result in similar microstructures near this interface. In contrast, the measured temperature rise in the GaN epilayer differs by $\sim 10\%$ between devices on 4H and 6H SiC substrate. This was con-

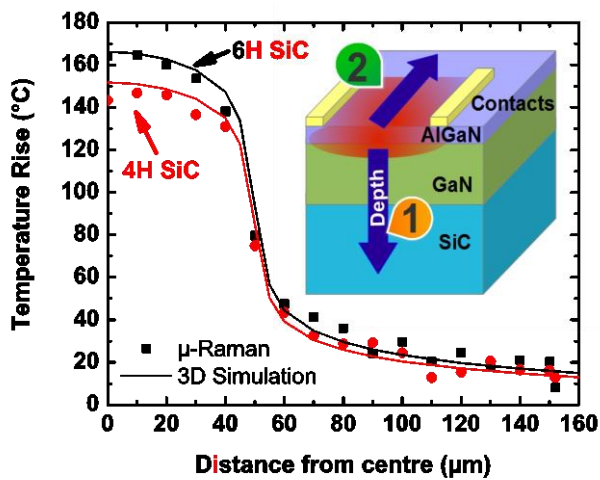


Figure 2 Lateral profile of temperature rise (with respect to EOC temperature) in GaN epilayer (dots) of two identical AlGaN/GaN devices on 6H SiC and 4H SiC, respectively, with operation conditions as in Fig. 1 and a standard temperature deviation of $\sim 2^\circ\text{C}$. Experimental results (dots) are overlaid with 3D thermal simulations (line), fitted to the experimental data with a fitting uncertainty of $\pm 0.1 \text{ W cm}^{-1} \text{ K}^{-1}$, which accounts for the deviation of the simulated profile to the experimental data. The inset illustrates the temperature scan across the device layer structure (1) and parallel to the contacts in the GaN epilayer (2).

firmly by measurements on multiple devices and dies. This difference indicates that device temperature in AlGaN/GaN HEMTs on 6H SiC is considerably higher than in devices on 4H SiC substrates. We note, this temperature represents the average temperature of the GaN layer. Consequently, the peak channel temperature difference will be greater.

To validate the results obtained from the vertical temperature profile and to quantify more accurately the thermal parameters by comparison with a thermal model, an additional temperature scan was performed laterally across the device, as illustrated in the inset of Fig. 2. The method labelled as (2) in the inset measures the GaN temperature from the centre of the device to outside the active device area. More details on this experimental approach can be found in Ref. 18. The measured temperature from the device centre, scanned parallel to the contact edges, is depicted in Fig. 2. Results from thermal simulations are overlaid.

A TBR_{eff} of $1.8 \times 10^{-8} \text{ m}^2 \text{ K W}^{-1}$ was used to account for the temperature rise at the GaN-SiC interface, which was found to be similar for both SiC substrates (as in Fig. 1), consistent with data reported in Ref. 12.

A thermal conductivity of $4.1 \text{ W cm}^{-1} \text{ K}^{-1}$ and $4.5 \text{ W cm}^{-1} \text{ K}^{-1}$ at room temperature was determined from a fitting to the experimental data obtained on devices on 6H SiC and 4H SiC, respectively, illustrating that 4H SiC is thermally favourable to 6H SiC. A temperature dependence of $T^{-1.5}$ was assumed in the fit of the thermal model to the experimental data, as commonly considered for SiC [13, 15].

Based on these thermal parameters determined, a thermal model for a $8 \times 125\text{-}\mu\text{m}$ -wide HEMT with a $30 \mu\text{m}$ gate pitch as well as similar structure and material parameters

was built. The difference in thermal conductivity between 4H and 6H SiC translates to a peak temperature rise in the AlGaN/GaN device channel near the gate contact edge of 89°C and 85°C for devices on 6H SiC and 4H SiC, respectively, assuming a 5 W/mm power dissipation. Note that the actual difference in peak temperatures will depend on the specific device structure, i.e., the numbers determined here are for this particular device structure, giving an example. Different thermal parameters, such as a higher TBR_{eff} , can enhance the impact of the SiC thermal conductivity difference. This temperature difference may not appear huge, however, is a factor to consider for the reliability of GaN-on-SiC devices, specifically with regard to the exponential relationship between lifetime and inverse of temperature. It is also of particular concern for accurate device thermal simulations, which lifetime testing methods and device design rely on. From a thermal management point of view, the results demonstrate that 4H SiC presents the substrate of choice under thermal considerations.

4 Conclusions

Identical AlGaN/GaN devices grown 6H SiC and 4H SiC, respectively, were studied by micro-Raman thermography to evaluate their thermal properties. A comparison with 3D thermal simulations revealed a 10% higher thermal conductivity for 4H SiC when compared to devices on 6H SiC, which, considering the exponential relationship between channel temperature and device lifetime, is beneficial for device reliability.

Acknowledgements The authors thank the Office of Naval Research and ONR Global (DRIFT program, monitored by Dr. Paul Maki) for financial support.

References

- [1] D. Runton, B. Trabert, J. Shealy, and R. Vetry, *IEEE Microwave Magazine* **14**, 82 (2013).
- [2] U. K. Mishra, L. Shen, T. E. Kazior, and Y.-F. Wu, *Proc. of the IEEE* **96**, 2, p. 287 (2008).
- [3] A. Sarua, Hangfeng Ji, M. Kuball M. J. Uren, T. Martin, K. P. Hilton, and R. S. Balmer, *IEEE Trans. Electron Devices* **53**, 10, p. 2438 (2006).
- [4] S. T. Sheppard, K. Doverspike, J. W. Pribble, S. T. Allen, J. W. Polmour, L. T. Kehias, and T. J. Jenkins, *IEEE Electron Device Lett.* **20**, 4, p. 161 (1999).
- [5] R. J. Trew, in *Proc. of the IEEE* **90**, 6, p. 1032 (2002).
- [6] E. A. Burgemeister, W. von Muench, and E. Pettenpaul, *J. Appl. Phys.* **50**, 9, p. 5790 (1979).
- [7] D. T. Morelli, J. P. Heremans, C. P. Beetz, W. S. Yoo, and H. Matsunami, *Appl. Phys. Lett.* **63**, 23, p. 3143 (1993).
- [8] G. A. Slack, *J. Appl. Phys.* **35**, 3460 (1964).
- [9] F. Cappelluti, M. Furno, A. Angelini, F. Bonani, M. Pirola, and G. Ghione, *IEEE Trans. Electron Devices* **54**, 7, p. 1744 (2007).
- [10] St. G. Müller, R. C. Glass, H. M. Hobgood, V. F. Tsvetkov, M. Brady, D. Henshall, D. Malta, R. Singh, J. Palmour, and C. H. Carter, Jr, *Materials Science and Engineering* **B80**, p. 327 (2001).

- [11]A. R. Powell and L. B. Rowland, in Proc. of the IEEE **90**, 6, p. 942 (2002).
- [12]A. Manoi, J. W. Pomeroy, N. Killat, and M. Kuball, IEEE Electron Device Lett. **31**, 12, p. 1395 (2010).
- [13]A. Sarua, Hangfeng Ji, K. P. Hilton, D. J. Wallis, M. J. Uren, T. Martin, and M. Kuball, IEEE Trans. Electron Devices **54**, 12, p. 3152 (2007).
- [14]G. J. Riedel, J. W. Pomeroy, K. P. Hilton, J. O. Maclean, D. J. Wallis, M. J. Uren, T. Martin, U. Forsberg, A. Lundskog, A. Kakanakova-Georgieva, G. Pozina, E. Janzén, R. Lossy, R. Pazirandeh, F. Brunner, J. Würfl, and M. Kuball, IEEE Electron Device Lett. **30**, 2, p. 103 (2009).
- [15]R. J. T. Simms, J. W. Pomeroy, M. J. Uren, T. Martin, and M. Kuball, IEEE Trans. Electron Devices **55**, 2, p. 478 (2008).
- [16]N Killat, T.-M. Chou, U. Chowdhury, J. Jimenez, and M. Kuball, in Proc. International Reliability Physics Symposium IRPS 2010, Anaheim, Los Angeles, USA.
- [17]J. Park, M. W. Shin, and C. C. Lee, IEEE Trans. Electron Devices **51**, 11, p. 1753 (2004).
- [18]J. Pomeroy, M. Bernardoni, D. C. Dumka, D. M. Fanning, and M. Kuball, Appl. Phys. Lett. **104**, 083513 (2014).